Cerebral Cortex October 2015;25:3527–3534
doi:10.1093/cercor/bhu194
Advance Access publication September 12, 2014

Structural Connectivity Networks of Transgender People

Andreas Hahn[1], Georg S. Kranz[1], Martin Küblböck[2], Ulrike Kaufmann[3], Sebastian Ganger[1], Allan Hummer[2], Rene Seiger[1], Marie Spies[1], Dietmar Winkler[1], Siegfried Kasper[1], Christian Windischberger[2], Dick F. Swaab[4] and Rupert Lanzenberger[1]

[1]Department of Psychiatry and Psychotherapy, [2]MR Center of Excellence, Center for Medical Physics and Biomedical Engineering, [3]Department of Obstetrics and Gynecology, Medical University of Vienna, Vienna, Austria and [4]Netherlands Institute for Neuroscience, Institute of the Royal Netherlands Academy of Arts and Sciences, Amsterdam, The Netherlands

Address correspondence to R. Lanzenberger, Functional, Molecular and Translational Neuroimaging Lab, Department of Psychiatry and Psychotherapy, Medical University of Vienna, Waehringer Guertel 18-20, 1090 Vienna, Austria. Email: rupert.lanzenberger@meduniwien.ac.at

Although previous investigations of transsexual people have focused on regional brain alterations, evaluations on a network level, especially those structural in nature, are largely missing. Therefore, we investigated the structural connectome of 23 female-to-male (FtM) and 21 male-to-female (MtF) transgender patients before hormone therapy as compared with 25 female and 25 male healthy controls. Graph theoretical analysis of whole-brain probabilistic tractography networks (adjusted for differences in intracranial volume) showed decreased hemispheric connectivity ratios of subcortical/limbic areas for both transgender groups. Subsequent analysis revealed that this finding was driven by increased interhemispheric lobar connectivity weights (LCWs) in MtF transsexuals and decreased intrahemispheric LCWs in FtM patients. This was further reflected on a regional level, where the MtF group showed mostly increased local efficiencies and FtM patients decreased values. Importantly, these parameters separated each patient group from the remaining subjects for the majority of significant findings. This work complements previously established regional alterations with important findings of structural connectivity. Specifically, our data suggest that network parameters may reflect unique characteristics of transgender patients, whereas local physiological aspects have been shown to represent the transition from the biological sex to the actual gender identity.

Keywords: graph theory, probabilistic tractography, structural connectivity, transgender

Introduction

The investigation of differences between men and women has been of great interest to the neuroscience community, as structural and functional aspects of the human brain show marked sex differences. This includes macroscopic features like differences in overall brain (Giedd et al. 2012) and lobar volumes (Allen et al. 2002), gray/white matter ratio and corpus callosum size (Leonard et al. 2008). On a regional level, such volumetric sex differences (Brun et al. 2009) reflect differential cognitive abilities between women and men regarding language and visuo-spatial processing (Gur et al. 1999). Investigations on gray and white matter microstructure showed further sex-specific differences when assessing gray matter volume (Chen et al. 2007; Luders et al. 2009), cortical thickness (Sowell et al. 2007), diffusivity metrics of major fiber tracts (Inano et al. 2013), volumes of subcortical cell groups (Swaab and Fliers 1985; Zhou et al. 1995) as well as neurochemical differences (Cosgrove et al. 2007) such as the serotonin transporter lateralization (Kranz et al. 2014). These structural findings are complemented by functional differences in neuronal activation (Schoning et al. 2007) as well as network characteristics of functional and structural connectivity (Biswal et al. 2010; Gong et al. 2011; Yan et al. 2011).

Our understanding of sex differences in the human brain is reflected in gender differences and endocrine influences in the prevalence and treatment of various psychiatric disorders (Bao and Swaab 2011). In this context, it is particularly interesting to study gender identity disorder. This disorder is characterized by the strong desire to belong to the gender opposite from their biological sex, which is often accompanied by emotional and social burden. Subsequently, patients often seek hormonal treatment and sex reassignment surgery in order to allow for more congruence between gender identity and appearance. This divergence between gender identity and biological sex has been proposed to emerge from the temporal difference between sexual differentiation of the genitals and the brain (Swaab and Garcia-Falgueras 2009; Bao and Swaab 2011). Specifically, the biological effect or lack of testosterone during 6–12 weeks of pregnancy leads to the formation of male or female sexual organs, respectively. In contrast, sexual differentiation of the brain occurs in the second half of pregnancy by organizing effects of sexual hormones. Hence, these developmental processes are independent and chronologically separated, so that masculinization of the genitals may not necessarily reflect that of the brain.

Accordingly, various studies report closer resemblance between transgender people and control subjects with the same gender identity than to those sharing their biological sex. This includes local differences in the number of neurons and volume of subcortical nuclei (Zhou et al. 1995; Garcia-Falgueras and Swaab 2008), functional alterations of regional cerebral blood blow (Nawata et al. 2010) and neuronal activation (Schoning et al. 2010) as well as structural differences of gray (Simon et al. 2013) and white matter microstructure (Rametti, Carrillo, Gomez-Gil, Junque, Segovia et al. 2011; Rametti, Carrillo, Gomez-Gil, Junque, Zubiarre-Elorza et al. 2011). Although transsexual people exhibit similar hormonal levels in adulthood as control subjects of the same biological sex, these studies indicate a transition of specific characteristics of their brains to the actual gender identity (i.e., feminization or masculinization).

In addition to the reported regional features, it is important to take into account characteristics of the human brain on a network level. Such connectivity analyses enable an investigation of interactions across brain regions and hence have provided valuable insights in fundamental human brain function

(Biswal et al. 2010), sex-specific differences (Gong et al. 2011; Tomasi and Volkow 2012), and psychiatric disorders (Broyd et al. 2009). However, to date only 1 case report (Santarnecchi et al. 2012) and 2 studies on functional connectivity are available (Ku et al. 2013; Lin et al. 2014), whereas structural networks of transsexual patients have not been assessed yet.

To address this issue, we investigated structural connectivity networks of female-to-male and male-to-female transsexuals as compared with healthy subjects. Applying graph theoretical analyses on networks obtained with probabilistic tractography, we evaluated global, hemispheric, lobar, and local connectivity metrics based on previously reported sex differences of the structural connectome (Gong et al. 2009; Ingalhalikar et al. 2014).

Methods

Subjects

In total, 94 subjects were included in this study. The sample comprised 23 female-to-male (FtM, mean age ± SD = 26.9 ± 7.1 years) and 21 male-to-female (MtF, 30.9 ± 8.4 years) transgender outpatients. For comparison, 25 healthy female (FC, 25.3 ± 6.2 years) and 25 male controls (MC, 25.6 ± 4.8 years) were included in the study. In transgender patients, diagnosis of gender identity disorder was assessed by the Structured Clinical Interview for the Diagnostic and Statistical Manual of Mental Disorders, 4th edition (DSM-IV) by an experienced psychiatrist at the screening visit. Briefly, this was diagnosed as a strong and persistent (>6 months) cross-gender identification and discomfort with the current sex, causing clinically significant distress or impairment in social, occupational, or other areas of functioning. Of note, the term gender identity disorder has changed to gender dysphoria in DSM-5 with a focus on dysphoria as a clinical problem (rather than the identity per se) and to avoid stigmatization. Transsexual subjects did not fulfill criteria for current comorbidities but 9 reported history of depression ($n = 2$), specific phobias ($n = 3$), obsessive compulsive disorder ($n = 1$), anorexia nervosa ($n = 2$), and substance abuse ($n = 4$). All patients reported subjective feelings to belong to the other gender before or at puberty, they wanted sex reassignment independent of study participation, and they underwent magnetic resonance imaging (MRI) scanning before onset of their hormonal treatment and surgery. All subjects underwent standard medical examinations with routine laboratory blood and pregnancy tests, electrocardiography, and assessment of general physical and neurological status. Exclusion criteria were presence or history of any severe physical or neurological disorders (and psychiatric disorders for healthy controls), substance abuse, intake of psychotropic medication and hormones (including contraceptives), pregnancy, and contraindications to MRI scanning. All subjects provided written informed consent after detailed explanation of the study protocol, and they were reimbursed for participation. This study was approved by the Ethics Committee of the Medical University of Vienna, and procedures were performed according to the Declaration of Helsinki.

Magnetic Resonance Imaging

All MRI measurements were obtained on a 3-Tesla scanner (Siemens Trio) using a 32-channel head coil. Diffusion-weighted images (DWIs) were acquired with a single-shot diffusion-weighted echo planar imaging sequence (TE/TR = 83/8700 ms, flip angle = 90°, image resolution 1.64 mm isotropic, b-value = 800 s/mm^2) in 30 diffusion-encoding directions and 1 non-diffusion-weighted b0-image. In addition, structural images were acquired in the same scanning session. Here, a T1-weighted magnetization-prepared rapid gradient echo sequence was used (TE/TR = 4.2/2300 ms, spatial resolution = 1.1 × 1 × 1 mm).

T1-Weighted Image Processing

Since men and women differ in overall brain size (Allen et al. 2002; Gong et al. 2009; Giedd et al. 2012), the total intracranial volume (TIV) was extracted from T1-weighted images for inclusion in the statistical analyses. Using the DARTEL module as implemented in the VBM8 toolbox (http://dbm.neuro.uni-jena.de/vbm/) for SPM8 (http://www.fil.ion.ucl.ac.uk/spm/), structural scans were individually segmented into gray and white matter as well as cerebrospinal fluid. The TIV was calculated as the sum of these 3 parameters.

Diffusion-Weighted Image Preprocessing and Tractography

Data preprocessing and tractography were carried out with the FMRIB software library (FSL v5.0.5, http://fsl.fmrib.ox.ac.uk/fsl/fslwiki/) using default parameters unless specified otherwise. This included adjustment for eddy currents as well as removal of the skull and nonbrain tissue with the brain extraction tool. Probabilistic tractography was done with FSL's Diffusion Toolbox in individual space (Behrens et al. 2003). First, local diffusion parameters were computed with 5000 sample streamlines and 2 fiber directions per voxel (Behrens et al. 2007). This enables modeling of crossing fibers and tracking of nondominant pathways. Second, whole-brain gray matter structural connectivity was computed using probabilistic tractography (matrix 3 mode). Here, sample streamlines are seeded from all voxels of the white matter, and a connection is detected if the streamline hits any 2 voxels of the gray matter target mask. Gray and white matter were given by an automated anatomical labeling-based gray matter atlas (Savli et al. 2012) and the DTI-81 white matter atlas (80% probability) of the International Consortium for Brain Mapping (ICBM) as provided in DiffeoMap, respectively. Of note, these atlases were only used for tractography, but not for the estimation of total brain volume (see T1-weighted image processing mentioned above). To register the 2 atlases to individual space, the ICBM T2-weighted image template was spatially normalized to each subject's b0-image and the transformation matrix was applied to the gray and white matter atlases. For computational reasons, the gray matter target mask was reduced to the perimeter voxels after transformation to individual space.

Connectivity Matrix and Graph Theoretical Parameters

For each subject, a weighted undirected (symmetric) structural connectivity matrix was constructed between the 89 gray matter regions of interest (ROIs) as described previously (Gong et al. 2009; Bozzali et al. 2011; Williams et al. 2013). Weighted networks are advantageous as the relation between different structural connections is preserved (instead of assigning equal weights to all tracts), and they are independent of network density thresholds (Gong et al. 2009; Rubinov and Sporns 2010). The connection probability P_{ij} between any 2 ROIs i and j was defined as the total number of streamlines connecting the 2 regions (S_{ij}) divided by the number of sampled streamlines (5000 per voxel). To adjust for differences in ROI size, this was further normalized by the surface area of the 2 regions (i.e., the number of voxels m_i and m_j):

$$P_{ij} = \frac{S_{ij}}{5000(m_i + m_j)}$$

To evaluate the structural network organization, graph theoretical analysis was applied, where a graph (network) can be represented by a set of nodes (brain regions), which are linked by edges (structural connections) (Bullmore and Sporns 2009). All graph theory metrics were computed for individual, non-thresholded, weighted connectivity matrices with the brain connectivity toolbox (Rubinov and Sporns 2010) in MatlabR2011a (MathWorks, Inc.), with parameters based on previous findings between men and women (Gong et al. 2009; Ingalhalikar et al. 2014). For comparison, and to rule out potential bias of our results, we also computed graph metrics for thresholded connectivity matrices within a range of sparsities (i.e., network densities) between 10% and 50% with 5% steps. Brain networks were visualized with Brain Net Viewer (Xia et al. 2013).

The network organization was evaluated at different levels, starting with global efficiency and small-worldness for an overall network assessment (Rubinov and Sporns 2010). The global efficiency describes how well the network is connected and is defined as the inverse of the

average (geodesic) shortest path length across all nodes. The composite parameter of small-worldness represents the ratio between the clustering coefficient (connectedness between adjacent nodes) and the shortest path length, both normalized by random network topology. Here, we used 100 random networks while preserving weight, strength, and degree distribution of the original network.

Next, structural connectivity networks were assessed at hemispheric and lobar levels by assigning the 89 ROIs to frontal, temporal, parietal, occipital, or subcortical/limbic lobes for the left and right hemisphere (Ingalhalikar et al. 2014). The hemispheric connectivity ratio (HCR) was calculated as the ratio between intra- and inter-hemispheric connection weights of a particular lobe. To further specify which connections drive differences in the HCR, the lobar connectivity weight (LCW) was computed. This is given as the sum of connection weights within (e.g., frontal left–frontal left) or between different lobes (e.g., frontal left–frontal right, frontal left–temporal left). Finally, the local efficiency was computed for a network evaluation at the regional level. Similar to the global efficiency, the local metric is the inverse of the average shortest path length between a single node and all other nodes.

Statistical Analyses

All statistics were computed in MatlabR2011a. To assess differences in overall brain size, a one-way analysis of variance (ANOVA) with 4 levels was calculated, followed by post hoc independent-samples *t*-tests between each of the groups. To compare graph metrics across groups, we applied random permutation testing to address the problem of multiple comparisons (Holmes et al. 1996; Nichols and Holmes 2002; Simpson et al. 2013; Ingalhalikar et al. 2014) with $N = 10000$ random permutations. This non-parametric method has the advantage of empirically deriving the distribution under the null hypothesis. Hence, it yields almost exact *P*-values with an (negligible) error of $1/N$ (Phipson and Smyth 2010; Simpson et al. 2013) and readily accounts for the multiple comparisons problem (Nichols and Holmes 2002). To assess statistical comparisons between the 4 population groups, the observed effect was first computed by an F-statistic (F_{observed}) for each network metric. For each permutation, subjects were then randomly assigned to any of the groups and the F-statistic was computed again (F_{permuted}). The *P*-value of the observed effect was finally calculated at a significance level $\alpha = 0.05$ as

$$P = \frac{n(F_{\text{permuted}} \geq F_{\text{observed}})}{N}$$

where N represents the number of permutations.

Significant effects were evaluated post hoc in the same manner using a t-statistic to assess which of the groups differ from each other. To exclude potential bias due to differences in brain size (Allen et al. 2002; Giedd et al. 2012), all statistical tests included TIV as nuisance covariate. Throughout the manuscript, superscript characters will be used to denote significant differences as compared with female controls (FC[a]), female-to-male transsexuals (FtM[b]), male controls (MC[c]), and male-to-female transsexuals (MtF[d]), with multiple characters indicating levels of significance ($^{a}P < 0.05$, $^{aa}P < 0.01$, $^{aaa}P < 0.001$).

Results

ANOVA indicated strong differences in TIV across the 4 groups ($F_{3,90} = 20.7$, $P < 10^{-9}$). Subsequent analysis showed lowest brain size for FC (TIV = 1344 ± 89mL[ccc,ddd]) and FtM (1344 ± 104mL[ccc,dd]), highest for MC (1546 ± 112mL[aaa,bbb,dd]), and intermediate for MtF (1453 ± 118mL[aaa,bb,cc]). Hence, the following results are reported after correcting for TIV.

Small-worldness was high for all 4 population groups, indicating good separation of structural networks from random topology. Global graph metrics were not significantly different between the 4 groups for small-worldness (FC = 2.96 ± 0.35, FtM = 3.10 ± 0.43, MC = 2.97 ± 0.41, MtF = 2.90 ± 0.38, $P = 0.15$) nor global efficiency (FC = 0.037 ± 0.008, FtM = 0.034 ± 0.009, MC = 0.037 ± 0.008, MtF = 0.041 ± 0.009, $P = 0.12$). In contrast, significant differences between the population groups were observed at the hemispheric, lobar, and regional levels (all $P < 0.05$).

More specifically, the HCR was lower in both transsexual patient groups as compared with healthy controls (subcortical/limbic right) and in MtF relative to the other groups (subcortical/limbic left, Table 1). Evaluating these differences at the lobar level, significant differences in LCW were found mostly for 1 of the transsexual patient groups (Table 1, Fig. 1). Interestingly, we observed that the above-mentioned differences in HCR were driven by increased interhemispheric lobar connectivity in MtF but decreased intrahemispheric lobar connectivity in FtM. More specifically, MtF showed increased LCW for connections between left subcortical/limbic and right frontal regions as well as for right subcortical/limbic to left frontal, temporal, and subcortical/limbic connections. On the other hand, FtM exhibited decreased LCW for right subcortical/limbic regions connecting to right frontal and temporal areas.

These findings were further reflected on a local level, where MtF exhibited significantly increased but FtM showed reduced local efficiencies in several brain regions (Table 2). Differences

Table 1
Structural connectivity differences in HCR and LCW

	FC[a]	FtM[b]	MC[c]	MtF[d]
Full and sparse matrices				
HCR				
Subc./limbic L	12.83 ± 6.41	11.01 ± 6.12	13.76 ± 8.33	**8.22 ± 3.04[aa,(b),c]**
Subc./limbic R	**10.66 ± 4.12[b,d]**	**8.51 ± 4.06[a,c]**	**11.95 ± 4.60[b,d]**	**8.37 ± 5.04[a,c]**
LCW				
Subc./limbic L–frontal R	0.14 ± 0.08	0.16 ± 0.10	0.15 ± 0.12	**0.26 ± 0.23[(a),cc]**
Subc./limbic L–parietal L	0.24 ± 0.10	0.24 ± 0.15	0.24 ± 0.13	**0.34 ± 0.17[(a),(b),c]**
Subc./limbic L–subc./limbic R	0.19 ± 0.13	0.21 ± 0.13	0.17 ± 0.11	**0.28 ± 0.14[aa,b,c]**
Subc./limbic R–frontal L	0.21 ± 0.10	0.21 ± 0.10	0.19 ± 0.11	**0.32 ± 0.21[a,(b),c]**
Subc./limbic R–frontal R	2.38 ± 0.69	**1.93 ± 0.67[aa,cc,d]**	2.44 ± 0.78	2.47 ± 0.87
Subc./limbic R–temporal R	0.73 ± 0.34	**0.51 ± 0.18[aa,cc,dd]**	0.73 ± 0.27[(d)]	0.84 ± 0.36[(c)]
Full matrices only				
LCW				
Subc./limbic R–temporal L	0.005 ± 0.008[(b)]	0.003 ± 0.005[(a)]	0.004 ± 0.006	**0.009 ± 0.011[b,c]**

Note: Full matrices are unthresholded; results from sparse (i.e., thresholded) matrices are considered if significance is observed in at least 7 of 9 levels of sparsity. Superscript characters indicate significant differences of 1 group as compared with female (FC[a]) or male controls (MC[b]), female-to-male (FtM[c]) or male-to-female transsexuals (MtF[d]).

Subc., subcortical; L, left; R, right; HCR, hemispheric connectivity ratio; LCW, lobar connectivity weight.

Bold values denote significance at $^{a}P < 0.05$, $^{aa}P < 0.01$, and $^{aaa}P < 0.001$; trends for statistical significance are denoted in brackets ([a]). If only 1 group shows significant differences, characters are only indicated there. Mean ± standard deviation represents raw values, whereas significant differences include correction for TIV.

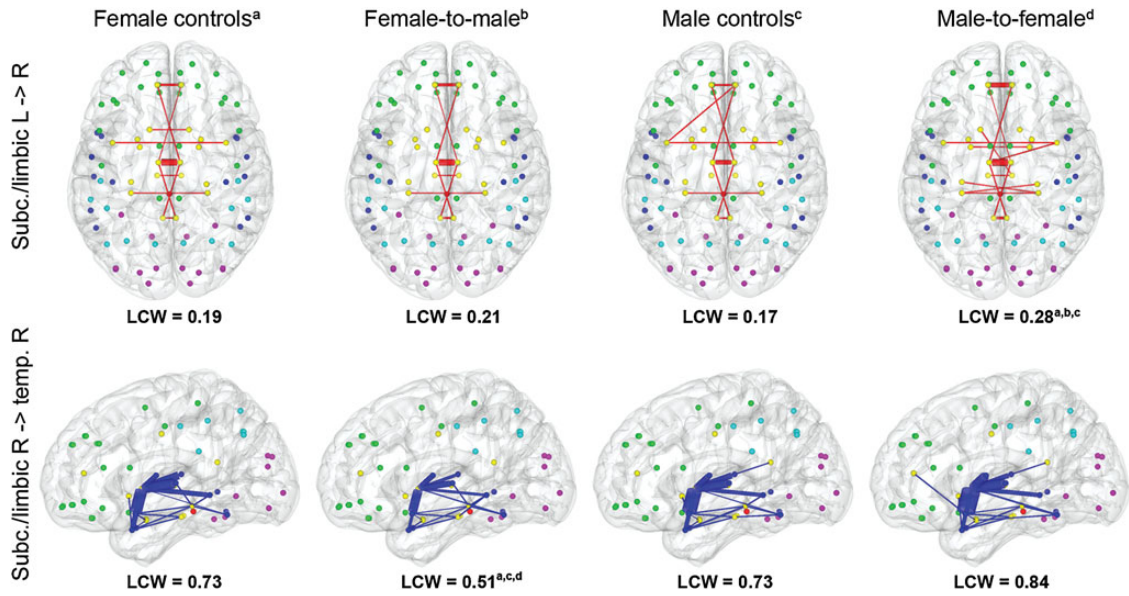

Figure 1. Average structural connectivity for female controls, female-to-male transsexuals, male controls, and male-to-female transsexuals for full (i.e., unthresholded connectivity matrices). Increased LCW was found in male-to-female transsexuals[a,b,c] between right subcortical (subc.)/limbic and left subcortical/limbic lobes (red, top). Decreased LCW was found in female-to-male transsexuals[a,c,d] between right subcortical/limbic and right temporal (temp.) lobes. Line thickness indicates connectivity weighting, whereas only connections with weights of >0.001 are shown (arbitrary choice to remove spurious connections as probabilistic tractography represents the robustness of the modeled tracts against noise). Nodes represent region of interest centers for frontal (green), temporal (blue), parietal (cyan), occipital (magenta), and limbic/subcortical brain regions (yellow). Characters indicate significant differences as compared with female controls (a), female-to-male transsexuals (b), male controls (c), or male-to-female transsexuals (d), see Table 1 for details. Axial images are in radiological view (i.e., left image side is right hemisphere).

between male and female controls were found mostly in areas of the right hemisphere, where males exhibited higher local efficiency (Table 2).

The above-mentioned results were replicated for thresholded connectivity matrices across a wide range of sparsities (i.e., at least 7 of 9 sparsity levels). Small-worldness (Fig. 2*A*) and global efficiency were not significantly different between groups (all $P > 0.05$). On the other hand, HCR was lower in both transsexual populations as compared with controls (subcortical/limibic right, Fig. 2*B*) and in MtF relative to the other groups (subcortical/limibic left). Similarly, LCW showed mostly significant differences for a single transsexual group, with increased LCW for MtF (Fig. 2*C*) and decreased LCW for FtM (Fig. 2*D*). For local efficiencies, FtM and MtF showed decreased and increased values for sparse matrices, respectively. However, different regions were identified depending on whether full or sparse matrices were used. Additional results are summarized in Tables 1 and 2.

Discussion

Here, we investigated the structural connectome of female-to-male and male-to-female transsexuals before hormonal treatment using graph theory. Compared with healthy controls, HCRs and LCWs showed differences specifically for connections between subcortical/limbic and cortical regions. The LCWs as well as local efficiencies further indicated a separation instead of a transition of the 2 transgender groups.

In line with previous results, we observed lower TIV for women as compared with men (Leonard et al. 2008; Giedd et al. 2012). Interestingly, FtM transsexuals exhibited similar TIV as female controls, whereas MtF transsexuals were in-between male and female healthy subjects. Despite this variation in overall brain size, none of the global network metrics differed between groups, each comprising similar efficiency and small-world properties. Such changes may simply cancel out on a global level as the evaluation of hemispheric, lobar, and regional metrics revealed widespread differences across groups. First of all, the decreased HCR of right (and to a lesser extent of left) subcortical/limbic brain regions was the only parameter separating patients from healthy controls, independent of their biological sex. It is, however, important to note that these differences emerged from contrary alterations between FtM and MtF transsexual people. More precisely, the intrahemispheric connections of subcortical/limbic to frontal and temporal areas were decreased in FtM patients as compared with all other groups. As there are currently no further studies of structural connectivity available in these patients, why FtM show a further decrease (rather than an expected increase) in intrahemispheric connectivity (Ingalhalikar et al. 2014) remains to be elucidated. On the other hand, increased interhemispheric connectivity between the subcortical/limbic and cortical regions mostly separated MtF transsexuals from the remaining subjects. Similar to the intermediate brain size of MtF patients, this might reflect a feminization as women exhibit stronger interhemispheric connections than men (Ingalhalikar et al. 2014). Interestingly, functional connectivity was also found to be increased in transsexuals as compared with controls (Ku et al. 2013; Lin et al. 2014); however, a separate analysis for the 2 patient groups is still missing.

Since subcortical and limbic brain regions are key elements in emotional processing and psychiatric disorders, one might be tempted to associate the specific alterations described here with the disease state of transsexual people (i.e., the divergence between the biological sex and gender identity). However, the different nature (intra- vs. inter-hemispheric) and direction (decreased vs. increased) between FtM and MtF

Table 2
Structural connectivity differences in local efficiency ($\times 10^{-3}$)

Local efficiency ($\times 10^{-3}$)	FC[a]	FtM[b]	MC[c]	MtF[d]
Full and sparse matrices				
Precentral gyrus L	5.0 ± 1.5[(c)]	5.2 ± 1.4	4.9 ± 1.7[(a)]	**6.4 ± 1.8[aa,b,c]**
Postcentral gyrus L	4.2 ± 1.3[(d)]	**4.1 ± 1.2[c,d]**	4.0 ± 1.3[(d)]	4.9 ± 1.4[(a),(c)]
Inferior occipital gyrus L	**1.4 ± 0.7[b,d]**	**1.1 ± 0.6[a,cc,ddd]**	**1.8 ± 1.0[bb]**	**2.0 ± 1.0[a,bbb]**
Insula R	10.5 ± 4.7	**6.8 ± 2.5[aaa,c,ddd]**	10.5 ± 4.5	11.4 ± 3.5
Inferior orbitofrontal cortex R	4.5 ± 2.6[(c)]	**3.1 ± 1.5[a,cc,dd]**	4.6 ± 2.1[(a)]	4.9 ± 1.9
Full matrices only				
Insula L	10.3 ± 3.9[(b),(d)]	**8.6 ± 3.4[(a),dd]**	**9.6 ± 3.5[d]**	**12.3 ± 3.7[(a),bb,c]**
Inferior frontal g., triang. L	3.9 ± 1.7[(c)]	3.7 ± 2.0[(c)]	3.9 ± 1.8[(a),(b),(d)]	**5.1 ± 1.9[a,b,(c)]**
Supplementary motor area L	5.8 ± 1.6	5.8 ± 2.1	5.2 ± 2.1	**7.2 ± 2.3[a,(b),cc]**
Paracentral gyrus L	3.8 ± 1.7	4.0 ± 1.4	3.2 ± 1.6	**4.7 ± 2.0[c]**
Precuneus L	6.7 ± 3.0	5.7 ± 2.9[(c)]	6.4 ± 2.8[(b)]	**8.2 ± 3.3[b,c]**
Supramarginal gyrus L	2.5 ± 0.6[(b)]	3.1 ± 1.9[(a)]	3.0 ± 1.1	**3.8 ± 1.5[aaa,b,c]**
Superior temporal gyrus L	3.6 ± 1.4	3.2 ± 1.5	3.6 ± 1.3	**4.8 ± 3.7[(a),b,cc]**
Inferior frontal g., triang. R	**4.4 ± 2.5[(b),c,(d)]**	**3.4 ± 1.9[(a),cc,dd]**	**4.4 ± 2.5[a,bb]**	**4.9 ± 2.0[(a),bb]**
Inferior frontal g., opercul. R	**3.7 ± 1.4[c,dd]**	**3.7 ± 0.2[(c),d]**	**4.0 ± 1.4[a,(b)]**	**4.6 ± 1.3[aa,b]**
Precentral gyrus R	**4.8 ± 1.6[c,dd]**	**4.5 ± 1.4[c,dd]**	**5.1 ± 1.5[a,b,(d)]**	**6.1 ± 1.8[aa,bb,(c)]**
Supramarginal gyrus R	**2.2 ± 0.7[cc,dd]**	**2.3 ± 1.3[c,d]**	**2.8 ± 1.1[aa,b]**	**3.2 ± 1.0[aa,b]**
Superior temporal gyrus R	3.7 ± 1.7	**2.7 ± 1.2[a,c,dd]**	3.6 ± 1.5[(d)]	4.4 ± 2.0[(c)]
Inferior occipital gyrus R	**1.3 ± 0.7[(b),c]**	**1.0 ± 0.5[(a),cc,d]**	**1.7 ± 0.9[a,bb,(d)]**	**1.4 ± 0.6[b,(c)]**
Sparse matrices only				
Lingual gyrus L	19.5 – 4.3	17.5 – 3.5	16.8 – 4.0	**23.9 – 5.6[(a),bb,c]**
Calcarine gyrus L	22.1 – 5.2[(b)]	20.8 – 4.3[(a),(c)]	20.8 – 4.9[(b)]	**32.0 – 6.6[(a),bb,c]**
Angular gyrus L	61.5 – 8.3	57.0 – 7.1	57.8 – 7.4	**74.1 – 10.4[b,c]**
Superior parietal gyrus L	57.9 – 6.7	**52.0 – 5.9[(c),d]**	57.7 – 6.3	69.3 – 8.8
Olfactory cortex R	54.2 – 6.3	**39.1 – 4.7[aa,(c),dd]**	53.7 – 5.9	61.6 – 7.3
Inferior temporal gyrus R	35.0 – 5.7	**26.0 – 4.3[a,c,dd]**	35.8 – 5.4	39.7 – 6.3
Middle temporal pole R	41.4 – 8.3	**37.8 – 6.4[a,d]**	48.9 – 7.4	58.5 – 8.7
Superior temporal pole R	58.9 – 8.7	**46.2 – 6.6[a,c,dd]**	63.0 – 8.4	72.6 – 9.2

Note: Full matrices are unthresholded; results from sparse (i.e., thresholded) matrices are considered if significance is observed in at least 7 of 9 levels of sparsity. Superscript characters indicate significant differences of 1 group as compared with female (FC[a]) or male controls (MC[b]), female-to-male (FtM[c]) or male-to-female transsexuals (MtF[d]).
Triang., triangular part; opercul., opercular part; L, left; R, right.
Bold values denote significance at $^{a}P < 0.05$, $^{aa}P < 0.01$, and $^{aaa}P < 0.001$, trends for statistical significance are denoted in brackets ([a]). If only 1 group shows significant differences, characters are only indicated there. Raw values are given as mean ± standard deviation (full matrices) and as mean for 10–50% sparsity (sparse matrices); significant differences include correction for TIV.

connectivity gives a more complex picture. That is, the observed differences may indicate that the strong desire to exhibit the opposite sex coupled with the psychological stress is accompanied by pronounced but distinct structural signatures for FtM and MtF, respectively. Again, the 2 patient groups also differed from control groups in their LCW, hence, exhibiting unique structural characteristics. A similar observation has been made for MtF transsexual patients as compared with male and female controls showing singular features of reduced thalamus and putamen volumes as well as increased gray matter volumes within the right insula and inferior frontal cortex (Savic and Arver 2011) (further discussed later). Although causal relationships cannot be established in this study, it is possible that similar to gender identity and sexual orientation, these structural differences in brain organization are also already determined during pregnancy (Bao and Swaab 2011). However, only a quarter of cases with gender problems during childhood convert to transsexuality in adulthood (Wallien and Cohen-Kettenis 2008). Hence, structural connections may alternatively differentiate during puberty, when the sexual organization of the brain is activated by sexual hormones (Phoenix et al. 1959; Swaab and Garcia-Falgueras 2009). This is supported by recent studies of structural connectivity, demonstrating profound re-wiring from childhood to adulthood (Dennis et al. 2013) and children showed markedly less pronounced gender differences than adolescents and adults (Ingalhalikar et al. 2014). The influence of the different hormones in males and females during puberty may also explain the opposite changes in structural connectivity between FtM and MtF observed here. This, however, remains an issue of future investigations, as sexual reversal of 2 important brain structures involved in sexual behavior (bed nucleus of stria terminalis and the interstitial nucleus of the anterior hypothalamus-3) was not influenced by circulating hormone levels neither in transsexual people nor in controls (Zhou et al. 1995; Kruijver et al. 2000; Garcia-Falgueras and Swaab 2008).

Investigating the brain on a network level adds important information to local structural and functional alterations in transsexual patients. In this context, previous results and interpretations of regional differences suggest a transition from the biological sex to the actual gender identity. Although feminization and masculinization indeed occurs, for example for neuronal cell number (Zhou et al. 1995; Kruijver et al. 2000; Garcia-Falgueras and Swaab 2008) and activation (Gizewski et al. 2009) as well as gray matter volume (Simon et al. 2013) and cortical thickness (Zubiaurre-Elorza et al. 2013), the identification of unique features of transsexual patients has been largely neglected in previous work. For instance, such an evaluation was impeded by the lack of both control groups in studies of cortical thickness (Luders et al. 2012), cerebral blood flow (Nawata et al. 2010) as well as functional MRI (Schoning et al. 2010) and connectivity (Ku et al. 2013). Other reports of white matter microstructure did not explicitly test for such unique differences of transsexual patients (Rametti, Carrillo, Gomez-Gil, Junque, Segovia et al. 2011; Rametti, Carrillo, Gomez-Gil, Junque, Zubiarre-Elorza et al. 2011). In contrast to the above-mentioned findings, a detailed evaluation of voxel-based morphometry and subcortical volumetric measures indicated no feminization of MtF transsexuals but rather a difference as compared with male and female controls (Savic

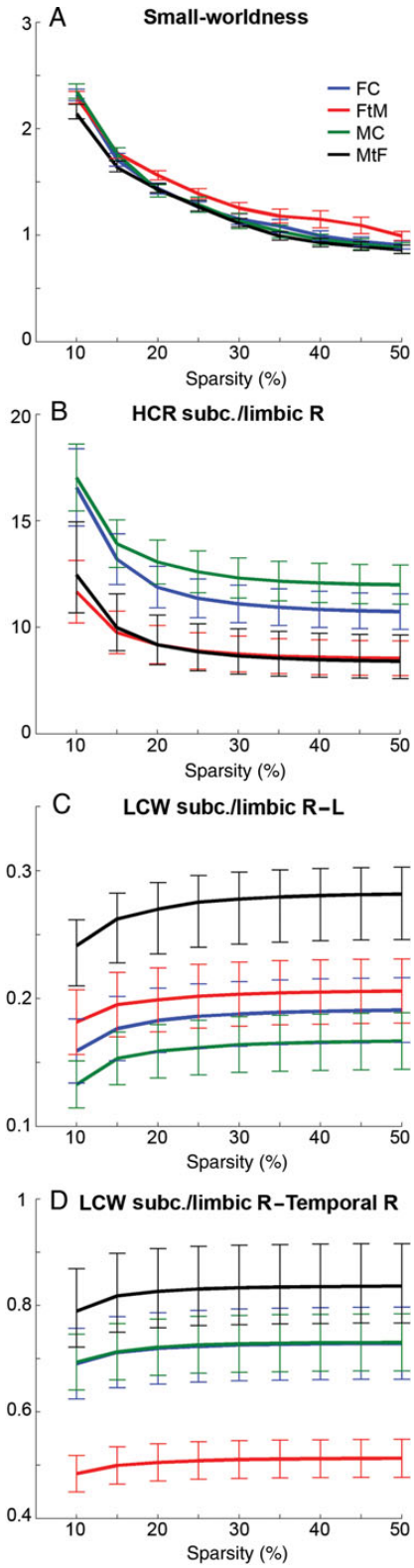

Figure 2. Average structural connectivity for female controls (FC, blue), female-to-male transsexuals (FtM, red), male controls (MC, green), and male-to-female transsexuals (MtF, black) for sparse connectivity matrices thresholded between 10 and 50% network density. Small-worldness was not significantly different between groups (*A*). In contrast, HCR of right subcortical/limbic connections separated patients from controls (*B*). The decreased HCR in transsexuals was caused by increased LCW in MtF (*C*) and decreased LCW in FtM (*D*). Values show mean ± standard error. See Table 1 for detailed statistics.

and Arver 2011). Similarly, the only study investigating functional connectivity networks in transsexuals with both control groups demonstrated unique differences of patients (although transition analysis was missing) (Lin et al. 2014). The notion that gender identity is an innate characteristic, which emerges from a particular brain structure (Cantor 2011), is further substantiated by the current study, where most structural network metrics represented unique differences as compared with healthy controls. Taken together, these observations suggest that most local physiological aspects indeed undergo a biological transition to the gender identity, whereas characteristics on a network level may reflect the psychological stress accompanied by the psychiatric disorder. Of note, further abnormalities of structural connectivity networks have already been described in other psychiatric conditions. For instance, patients with major depressive disorder exhibited decreased structural connectivity within the default mode network as well as frontal and subcortical brain regions (Korgaonkar et al. 2014). Similarly, schizophrenic patients showed reduced overall network efficiencies and nodal degree as well as impairment of a specific fronto-parietal/occipital network (Zalesky et al. 2011).

For the regional network feature of local efficiency, we observed further singular differences of transsexual patients especially for the insular cortex. Importantly, the insula is activated during sexual arousal (Arnow et al. 2002; Karama et al. 2002) and its dysfunction is related to sexual behavior abnormalities (Miller et al. 1986) and bodily self-consciousness (Heydrich and Blanke 2013). Moreover, its functional connections with the cingulate cortex may code for integration of emotional information into a subjective representation of the body (Taylor et al. 2009), corroborating the relevance of the insula in sexual identity. On the other hand, we also found areas such as the right precentral and supramarginal gyri separating biological males from females (Gong et al. 2009), which was independent of gender identity. Still, differences between male and female controls were less pronounced than for transsexual patients. This is in line with a previous report of rather few sex differences (Dennis et al. 2013), which might be attributable to a substantial overlap between men and women as demonstrated earlier (Gong et al. 2009). Such an overlap further explains the missing replication of previous sex differences in hemispheric and lobar connectivity (Ingalhalikar et al. 2014). The latter issue may, however, be also related to methodological differences such as sample size, age range, and correction for brain size, where another study also did not observe sex differences in interhemispheric connections (Dennis et al. 2013). Of note, the usage of non-thresholded or sparse matrices influenced the results on local but not macroscopic graph metrics. That is, several regions exhibited significant differences in local efficiency either for full or sparse matrices. We speculate that this effect might be related to increased noise at the regional level, which may cancel out for macroscopic parameters as these yielded stable results independent of the sparsity. Accordingly, a recent test–retest assessment of structural connectivity metrics reported better reproducibility for global than for local metrics (Owen et al. 2013). Taken together, it seems that macroscopic parameters offer reliable metrics for the assessment of group differences, whereas local ones should be interpreted with greater caution. Another limitation is that transsexual subjects did not provide

exact dates when they experienced to belong to the other gender; hence, the evaluation of potential associations with the obtained network metrics will remain an issue for future research.

Conclusions

Investigating structural networks in female-to-male and male-to-female transsexuals, we observed differences in hemispheric and lobar connectivity as well as local efficiencies when compared with healthy controls. Previously reported regional characteristics of transsexual patients mostly represent the transition of the biological sex to the actual gender identity. Hence, our interregional findings add valuable complementary information as the evaluation on a network level revealed unique features, which seem to be specific for each of the patient groups.

Funding

This research was supported by a grant of the Austrian Science Fund (FWF P23021) to RL. Funding to pay the Open Access publication charges for this article was provided by the Austrian Science Fund (FWF).

Notes

Conflict of interest: None declared.

References

Allen JS, Damasio H, Grabowski TJ. 2002. Normal neuroanatomical variation in the human brain: an MRI-volumetric study. Am J Phys Anthropol. 118:341–358.

Arnow BA, Desmond JE, Banner LL, Glover GH, Solomon A, Polan ML, Lue TF, Atlas SW. 2002. Brain activation and sexual arousal in healthy, heterosexual males. Brain. 125:1014–1023.

Bao AM, Swaab DF. 2011. Sexual differentiation of the human brain: relation to gender identity, sexual orientation and neuropsychiatric disorders. Front Neuroendocrinol. 32:214–226.

Behrens TE, Berg HJ, Jbabdi S, Rushworth MF, Woolrich MW. 2007. Probabilistic diffusion tractography with multiple fibre orientations: what can we gain? Neuroimage. 34:144–155.

Behrens TE, Woolrich MW, Jenkinson M, Johansen-Berg H, Nunes RG, Clare S, Matthews PM, Brady JM, Smith SM. 2003. Characterization and propagation of uncertainty in diffusion-weighted MR imaging. Magn Reson Med. 50:1077–1088.

Biswal BB, Mennes M, Zuo X-N, Gohel S, Kelly C, Smith SM, Beckmann CF, Adelstein JS, Buckner RL, Colcombe S et al. 2010. Toward discovery science of human brain function. Proc Natl Acad Sci USA. 107:4734–4739.

Bozzali M, Parker GJ, Serra L, Embleton K, Gili T, Perri R, Caltagirone C, Cercignani M. 2011. Anatomical connectivity mapping: a new tool to assess brain disconnection in Alzheimer's disease. Neuroimage. 54:2045–2051.

Broyd SJ, Demanuele C, Debener S, Helps SK, James CJ, Sonuga-Barke EJS. 2009. Default-mode brain dysfunction in mental disorders: a systematic review. Neurosci Biobehav Rev. 33:279–296.

Brun CC, Lepore N, Luders E, Chou YY, Madsen SK, Toga AW, Thompson PM. 2009. Sex differences in brain structure in auditory and cingulate regions. Neuroreport. 20:930–935.

Bullmore E, Sporns O. 2009. Complex brain networks: graph theoretical analysis of structural and functional systems. Nat Rev Neurosci. 10:186–198.

Cantor JM. 2011. New MRI studies support the Blanchard typology of male-to-female transsexualism. Arch Sex Behav. 40:863–864.

Chen X, Sachdev PS, Wen W, Anstey KJ. 2007. Sex differences in regional gray matter in healthy individuals aged 44–48 years: a voxel-based morphometric study. Neuroimage. 36:691–699.

Cosgrove KP, Mazure CM, Staley JK. 2007. Evolving knowledge of sex differences in brain structure, function, and chemistry. Biol Psychiatry. 62:847–855.

Dennis EL, Jahanshad N, McMahon KL, de Zubicaray GI, Martin NG, Hickie IB, Toga AW, Wright MJ, Thompson PM. 2013. Development of brain structural connectivity between ages 12 and 30: a 4-Tesla diffusion imaging study in 439 adolescents and adults. Neuroimage. 64:671–684.

Garcia-Falgueras A, Swaab DF. 2008. A sex difference in the hypothalamic uncinate nucleus: relationship to gender identity. Brain. 131:3132–3146.

Giedd JN, Raznahan A, Mills KL, Lenroot RK. 2012. Review: magnetic resonance imaging of male/female differences in human adolescent brain anatomy. Biol Sex Differ. 3:19.

Gizewski ER, Krause E, Schlamann M, Happich F, Ladd ME, Forsting M, Senf W. 2009. Specific cerebral activation due to visual erotic stimuli in male-to-female transsexuals compared with male and female controls: an fMRI study. J Sex Med. 6:440–448.

Gong G, He Y, Evans AC. 2011. Brain connectivity: gender makes a difference. Neuroscientist. 17:575–591.

Gong G, Rosa-Neto P, Carbonell F, Chen ZJ, He Y, Evans AC. 2009. Age- and gender-related differences in the cortical anatomical network. J Neurosci. 29:15684–15693.

Gur RC, Turetsky BI, Matsui M, Yan M, Bilker W, Hughett P, Gur RE. 1999. Sex differences in brain gray and white matter in healthy young adults: correlations with cognitive performance. J Neurosci. 19:4065–4072.

Heydrich L, Blanke O. 2013. Distinct illusory own-body perceptions caused by damage to posterior insula and extrastriate cortex. Brain. 136:790–803.

Holmes AP, Blair RC, Watson JD, Ford I. 1996. Nonparametric analysis of statistic images from functional mapping experiments. J Cereb Blood Flow Metab. 16:7–22.

Inano S, Takao H, Hayashi N, Yoshioka N, Mori H, Kunimatsu A, Abe O, Ohtomo K. 2013. Effects of age and gender on neuroanatomical volumes. J Magn Reson Imaging. 37:1072–1076.

Ingalhalikar M, Smith A, Parker D, Satterthwaite TD, Elliott MA, Ruparel K, Hakonarson H, Gur RE, Gur RC, Verma R. 2014. Sex differences in the structural connectome of the human brain. Proc Natl Acad Sci USA. 111:823–828.

Karama S, Lecours AR, Leroux JM, Bourgouin P, Beaudoin G, Joubert S, Beauregard M. 2002. Areas of brain activation in males and females during viewing of erotic film excerpts. Hum Brain Mapp. 16:1–13.

Korgaonkar MS, Fornito A, Williams LM, Grieve SM. 2014. Abnormal structural networks characterize major depressive disorder: a connectome analysis. Biol Psychiatry. doi:10.1016/j.biopsych.2014.02.018.

Kranz GS, Hahn A, Baldinger P, Haeusler D, Philippe C, Kaufmann U, Wadsak W, Savli M, Hoeflich A, Kraus C et al. 2014. Cerebral serotonin transporter asymmetry in females, males and male-to-female transsexuals measured by PET in vivo. Brain Struct Funct. 219:171–183.

Kruijver FP, Zhou JN, Pool CW, Hofman MA, Gooren LJ, Swaab DF. 2000. Male-to-female transsexuals have female neuron numbers in a limbic nucleus. J Clin Endocrinol Metab. 85:2034–2041.

Ku HL, Lin CS, Chao HT, Tu PC, Li CT, Cheng CM, Su TP, Lee YC, Hsieh JC. 2013. Brain signature characterizing the body-brain-mind axis of transsexuals. PloS One. 8:e70808.

Leonard CM, Towler S, Welcome S, Halderman LK, Otto R, Eckert MA, Chiarello C. 2008. Size matters: cerebral volume influences sex differences in neuroanatomy. Cereb Cortex. 18:2920–2931.

Lin CS, Ku HL, Chao HT, Tu PC, Li CT, Cheng CM, Su TP, Lee YC, Hsieh JC. 2014. Neural network of body representation differs between transsexuals and cissexuals. PloS One. 9:e85914.

Luders E, Gaser C, Narr KL, Toga AW. 2009. Why sex matters: brain size independent differences in gray matter distributions between men and women. J Neurosci. 29:14265–14270.

Luders E, Sanchez FJ, Tosun D, Shattuck DW, Gaser C, Vilain E, Toga AW. 2012. Increased cortical thickness in male-to-female transsexualism. J Behav Brain Sci. 2:357–362.

Miller BL, Cummings JL, McIntyre H, Ebers G, Grode M. 1986. Hypersexuality or altered sexual preference following brain injury. J Neurol Neurosurg Psychiatry. 49:867–873.

Nawata H, Ogomori K, Tanaka M, Nishimura R, Urashima H, Yano R, Takano K, Kuwabara Y. 2010. Regional cerebral blood flow changes in female to male gender identity disorder. Psychiatry Clin Neurosci. 64:157–161.

Nichols TE, Holmes AP. 2002. Nonparametric permutation tests for functional neuroimaging: a primer with examples. Hum Brain Mapp. 15:1–25.

Owen JP, Ziv E, Bukshpun P, Pojman N, Wakahiro M, Berman JI, Roberts TP, Friedman EJ, Sherr EH, Mukherjee P. 2013. Test-retest reliability of computational network measurements derived from the structural connectome of the human brain. Brain Connect. 3:160–176.

Phipson B, Smyth GK. 2010. Permutation *P*-values should never be zero: calculating exact *P*-values when permutations are randomly drawn. Stat Appl Genet Mol Biol. 9:Article39.

Phoenix CH, Goy RW, Gerall AA, Young WC. 1959. Organizing action of prenatally administered testosterone propionate on the tissues mediating mating behavior in the female guinea pig. Endocrinology. 65:369–382.

Rametti G, Carrillo B, Gomez-Gil E, Junque C, Segovia S, Gomez A, Guillamon A. 2011. White matter microstructure in female to male transsexuals before cross-sex hormonal treatment. A diffusion tensor imaging study. J Psychiatr Res. 45:199–204.

Rametti G, Carrillo B, Gomez-Gil E, Junque C, Zubiarre-Elorza L, Segovia S, Gomez A, Guillamon A. 2011. The microstructure of white matter in male to female transsexuals before cross-sex hormonal treatment. A DTI study. J Psychiatr Res. 45:949–954.

Rubinov M, Sporns O. 2010. Complex network measures of brain connectivity: uses and interpretations. Neuroimage. 52:1059–1069.

Santarnecchi E, Vatti G, Dettore D, Rossi A. 2012. Intrinsic cerebral connectivity analysis in an untreated female-to-male transsexual subject: a first attempt using resting-state fMRI. Neuroendocrinology. 96:188–193.

Savic I, Arver S. 2011. Sex dimorphism of the brain in male-to-female transsexuals. Cereb Cortex. 21:2525–2533.

Savli M, Bauer A, Mitterhauser M, Ding YS, Hahn A, Kroll T, Neumeister A, Haeusler D, Ungersbock J, Henry S et al. 2012. Normative database of the serotonergic system in healthy subjects using multitracer PET. NeuroImage. 63:447–459.

Schoning S, Engelien A, Bauer C, Kugel H, Kersting A, Roestel C, Zwitserlood P, Pyka M, Dannlowski U, Lehmann W et al. 2010. Neuroimaging differences in spatial cognition between men and male-to-female transsexuals before and during hormone therapy. J Sex Med. 7:1858–1867.

Schoning S, Engelien A, Kugel H, Schafer S, Schiffbauer H, Zwitserlood P, Pletziger E, Beizai P, Kersting A, Ohrmann P et al. 2007. Functional anatomy of visuo-spatial working memory during mental rotation is influenced by sex, menstrual cycle, and sex steroid hormones. Neuropsychologia. 45:3203–3214.

Simon L, Kozak LR, Simon V, Czobor P, Unoka Z, Szabo A, Csukly G. 2013. Regional grey matter structure differences between transsexuals and healthy controls – a voxel based morphometry study. PloS One. 8:e83947.

Simpson SL, Lyday RG, Hayasaka S, Marsh AP, Laurienti PJ. 2013. A permutation testing framework to compare groups of brain networks. Front Comput Neurosci. 7:171.

Sowell ER, Peterson BS, Kan E, Woods RP, Yoshii J, Bansal R, Xu D, Zhu H, Thompson PM, Toga AW. 2007. Sex differences in cortical thickness mapped in 176 healthy individuals between 7 and 87 years of age. Cereb Cortex. 17:1550–1560.

Swaab DF, Fliers E. 1985. A sexually dimorphic nucleus in the human brain. Science. 228:1112–1115.

Swaab DF, Garcia-Falgueras A. 2009. Sexual differentiation of the human brain in relation to gender identity and sexual orientation. Funct Neurol. 24:17–28.

Taylor KS, Seminowicz DA, Davis KD. 2009. Two systems of resting state connectivity between the insula and cingulate cortex. Hum Brain Mapp. 30:2731–2745.

Tomasi D, Volkow ND. 2012. Gender differences in brain functional connectivity density. Hum Brain Mapp. 33:849–860.

Wallien MSC, Cohen-Kettenis PT. 2008. Psychosexual outcome of gender-dysphoric children. J Am Acad Child Adolesc Psychiatry. 47:1413–1423.

Williams VJ, Juranek J, Stuebing K, Cirino PT, Dennis M, Fletcher JM. 2013. Examination of frontal and parietal tectocortical attention pathways in spina bifida meningomyelocele using probabilistic diffusion tractography. Brain Connect. 3:512–522.

Xia M, Wang J, He Y. 2013. BrainNet Viewer: a network visualization tool for human brain connectomics. PloS One. 8:e68910.

Yan C, Gong G, Wang J, Wang D, Liu D, Zhu C, Chen ZJ, Evans A, Zang Y, He Y. 2011. Sex- and brain size-related small-world structural cortical networks in young adults: a DTI tractography study. Cereb Cortex. 21:449–458.

Zalesky A, Fornito A, Seal ML, Cocchi L, Westin CF, Bullmore ET, Egan GF, Pantelis C. 2011. Disrupted axonal fiber connectivity in schizophrenia. Biol Psychiatry. 69:80–89.

Zhou JN, Hofman MA, Gooren LJ, Swaab DF. 1995. A sex difference in the human brain and its relation to transsexuality. Nature. 378:68–70.

Zubiaurre-Elorza L, Junque C, Gomez-Gil E, Segovia S, Carrillo B, Rametti G, Guillamon A. 2013. Cortical thickness in untreated transsexuals. Cereb Cortex. 23:2855–2862.